Arch. Pharm. Res.
https://doi.org/10.1007/s12272-022-01412-3

Online ISSN 1976-3786
Print ISSN 0253-6269

Archives of Pharmacal Research
www.springer.com/12272

RESEARCH ARTICLE

Inhibition of autophagy with chloroquine dysregulates mitochondrial quality control and energetics in adipocytes

Hafiz Muhammad Ahmad Javaid[1] · Hwayeon Lim[2] · Sooim Shin[2,3] · Joo Young Huh[1]

Received: 15 July 2022 / Accepted: 17 October 2022

Abstract Autophagy is a complex degradation pathway through which damaged or dysfunctional proteins and organelles are removed. Its pharmacological modulators have been extensively used in a wide range of basic research and preclinical studies. However, the effects of these inhibitors on metabolism, in addition to autophagy inhibition, are not fully elucidated. Chloroquine is a clinically relevant compound that inhibits autophagy by preventing the fusion of autophagosomes with lysosomes. In this study, we aimed to examine the effect of chloroquine on mitochondrial quality control and respiratory function by utilizing 3T3-L1 mouse adipocytes treated with chloroquine at various time points. We found that chloroquine could disturb genes related to mitochondrial fission, biogenesis, and mitophagy, leading to mitochondrial DNA damage. Although the inhibition of autophagy by chloroquine resulted in an increased prohibitin expression, respiratory function was downregulated in a time-dependent manner. Moreover, chloroquine treatment induced oxidative stress, apoptosis, and metabolic dysregulation. These data demonstrated that chloroquine significantly affected mitochondrial respiratory function and metabolism, which was consistent with impaired mitochondrial quality associated with autophagy inhibition.

Keywords Obesity · Adipocytes · Mitochondria · Autophagy · Chloroquine

Introduction

Obesity is described as excessive fat buildup in adipose tissues, leading to a cluster of disorders known as "metabolic syndrome", including insulin resistance, type 2 diabetes, and cardiovascular disease (Van Gaal et al. 2006). The pathogenesis of obesity-induced metabolic disease is complex because it involves alterations in metabolic, immune, and endocrine functions in adipocytes and adipose tissues (Kahn et al. 2019). Recent research showed autophagy dysregulation in obesity is involved in the regulation of the metabolic and immune functions of adipose tissues, leading to the progression of metabolic disorders (Namkoong et al. 2018). Autophagy is an intracellular defense mechanism to maintain homeostasis by clearing damaged and dysfunctional organelles (Klionsky and Emr 2000). Previous studies on adipocytes revealed that autophagy is largely involved in adipocyte differentiation through which autophagy inhibition hampers adipogenesis (Zhang et al. 2013). Conversely, the role of autophagy in mature adipocytes has yet to be fully defined. Notably, autophagy is altered in adipose tissues in individuals with obesity, but whether the related autophagy

Sooim Shin and Joo Young Huh have contributed equally to this work.

Supplementary Information The online version contains supplementary material available at https://doi.org/10.1007/s12272-022-01412-3.

✉ Sooim Shin
sooim.shin@jnu.ac.kr

✉ Joo Young Huh
jooyhuh@jnu.ac.kr

[1] College of Pharmacy, Chonnam National University, 77, Yongbong-ro, Buk-gu, Gwangju 61186, Republic of Korea

[2] Department of Bioengineering and Biotechnology, College of Engineering, Chonnam National University, 77 Yongbong-ro, Buk-gu, 61186 Gwangju, Republic of Korea

[3] Interdisciplinary Program of Bioenergy and Biomaterials Graduate School, College of Engineering, Chonnam National University, 77 Yongbong-ro, Buk-gu, Gwangju 61186, Republic of Korea

Published online: 28 October 2022

activity is increased or impaired remains debatable (Clemente-Postigo et al. 2020).

Mitochondria are critical integrators of energy production, reactive oxygen species (ROS) generation, signaling transduction, and apoptosis (Galluzzi et al. 2012). Increasing evidence has shown that mitochondrial malfunction is a pivotal event in disturbing cellular homeostasis and metabolic adaptation (Bhatti et al. 2017). Mitochondrial homeostasis is achieved by balancing mitochondrial biosynthesis and degradation (Altshuler-Keylin and Kajimura 2017). While several transcriptional regulators, including peroxisome proliferator-activated receptor gamma coactivator-1 alpha (PGC1α), have been identified as regulators of mitochondrial biogenesis (LeBleu et al. 2014), the removal of dysfunctional or unneeded mitochondria relies on mitophagy, which is a unique autophagy targeting dysfunctional mitochondria (Ashrafi and Schwarz 2013). Damaged mitochondria are detected by PTEN-induced putative kinase (PINK1) and Parkin and engulfed by autophagosomes for subsequent catabolism by lysosomes (McWilliams and Muqit, 2017). Conversely, the inhibition of mitophagy-mediated mitochondrial clearance is beneficial to metabolism by enhancing the transition from white adipocytes to beige adipocytes and the thermogenic capacity in diet-induced obesity (Altshuler-Keylin et al. 2016). Given the complex role of autophagy on mitochondrial homeostasis, further investigation into the relationship between autophagy and mitochondria should be performed in terms of metabolic regulation in adipocytes.

Various pharmacological inhibitors of autophagy have been widely used to provide insights into the protective and deleterious effects of autophagy (Galluzzi et al. 2017). Among them, chloroquine is a lysosomotropic weak base that neutralizes intra-lysosomal acidity and hence arrests autophagy by preventing the fusion of autophagosomes with lysosomes (Mauthe et al. 2018). Chloroquine is used as an FDA-approved drug for malaria therapy in clinical settings (Coban 2020) and debated for its potential use in COVID-19 treatment (Zou et al. 2020). In addition to the effects of chloroquine on autophagy inhibition, the influence of chloroquine on mitochondrial homeostasis in adipocytes remains unexplored. Thus, identifying the time-dependent effect of chloroquine on mitochondrial quality control and energetics in adipocytes may enhance our understanding of the utilization of autophagy inhibitors for studying the mechanistic link between autophagy, mitochondria, and metabolism.

In this study, we hypothesized that the pharmacological inhibition of autophagy by chloroquine in adipocytes altered the mitochondrial quality control machinery, thereby impairing adipocyte metabolism. We found that chloroquine-treated adipocytes presented dysfunctional mitochondria with decreased respiratory functions. As a result, redox homeostasis was disrupted, and apoptotic activity was enhanced. In these adipocytes, glucose uptake and lipid metabolism were impaired, suggesting that chloroquine-mediated autophagy inhibition affected mitochondrial integrity, thus leading to adipocyte dysregulation.

Materials and methods

3T3-L1 culture and treatment

3T3-L1 cells (ATCC, Manassas, VA, USA) were cultured as previously described (Javaid et al. 2021). Briefly, preadipocytes were cultured in high-glucose Dulbecco's modified Eagle medium (DMEM; Gibco, Carlsbad, CA, USA) supplemented with 10% fetal bovine serum (FBS; HyClone; Logan, UT, USA) and 1% penicillin/streptomycin and incubated at 37 °C with 5% CO_2. Two days after reaching 100% confluency (day 0), the cells were incubated in differentiation media containing insulin, dexamethasone, 3-isobutyl-1-methylxanthine, and rosiglitazone. On day 8, mature adipocytes were treated with 30 μM chloroquine (C6628, Sigma; Saint Louis, MO, USA) for subsequent experiments.

Oxygen consumption rate

Briefly, 3T3-L1 cells were grown and differentiated in XFe96 well plates coated with gelatin. On the assay day, the cell culture medium was changed to Seahorse XF DMEM supplemented with 1 mM pyruvate, 2 mM glutamate, and 10 mM glucose. The plate was incubated in a non-CO_2 incubator at 37 °C for 1 h after oligomycin (2 μM), FCCP (2 μM), and rotenone/antimycin (1 μM) were added to their respective ports prior to the assay. After cartridge calibration, the cells were placed in XFe96 analyzer (Agilent Seahorse Bioscience, Santa Clara, CA, USA) to measure the oxygen consumption rate.

Oxidative stress measurement

Hydrogen peroxide was measured using a commercially available ROS-Glo H_2O_2 assay kit (G8820, Promega; Madison, WI, USA) in accordance with the manufacturer's instructions. Briefly, after the cells were treated, H_2O_2 substrate was added in the last 6 h of treatment at a final concentration of 25 μM. ROS-Glo detection reagent was added to measure luminescence by using a microplate reader.

Caspase-3 activity assay

Caspase-3 activity in cells was measured using a commercially available Caspase-Glo 3/7 assay kit (G8090, Promega) in accordance with the manufacturer's instructions. Briefly, after the cells were treated, caspase-3 reagent was added to

each well, and luminescence was measured using a microplate reader.

Glucose uptake assay

Glucose uptake was measured using a commercially available Glucose Uptake-Glo assay kit (J1341, Promega) in accordance with the manufacturer's instructions. After the cells were treated, the medium was removed and washed with PBS to remove any glucose. After 1 mM 2-deoxyglucose (2DG) was added per well, the plate was incubated at room temperature for 10 min. Stop buffer and neutralization buffer were sequentially added. Then, 2-deoxyglucose-6-phosphate (2DG6P) detection reagent was added, and luminescence was measured using a microplate reader.

Antioxidant activity assay

Total glutathione (GSH) level was determined using a GSH assay kit (CS0260, Sigma). Lysate (20 μg) was treated with 5% (w/v) sulfosalicylic acid at 4 °C for 10 min and centrifugated at 10,000 × *g* for 10 min. The supernatant and standard solution (40 μl) were transferred to 96-well plates, and 150 μl working solution was added. After 5 min of incubation at room temperature, 50 μl of the reduced nicotinamide adenine dinucleotide phosphate (NADPH) was added to each well, and the change in the absorbance of 5,5′-dithiobis-2-nitrobenzoic acid (DTNB) was monitored at 412 nm induced by glutathione oxidation. GSH level was calculated in accordance with the manufacturer's instructions.

Total superoxide dismutase (SOD) activity was determined using a superoxide dismutase activity assay kit (ab65354; Abcam, Cambridge, UK). Lysate (10 μg) was mixed with water-soluble tetrazolium salt (WST-1) working solution and enzyme working solution and incubated at 37 °C for 20 min. SOD inhibited the reduction of WST-1, and the inhibition rate of WST-1 reduction was calculated as the SOD activity. To further detect MnSOD activity, 2 mM potassium cyanide was added at 37 °C for 40 min to inhibit Cu/ZnSOD (Traba et al. 2017). The absorbance of WST-1 formazan, which is a form of reduced WST-1, was monitored at 450 nm by using SpectraMax iD3 (Molecular Devices, San Jose, CA, USA), and each absorbance was subtracted by initial absorbance.

Oil Red O staining

Preadipocytes and mature adipocytes were fixed with 10% formalin for 30 min. A stock solution of 0.5% Oil Red O solution (00625, Sigma) was prepared in isopropranolol, filtered, and diluted with distilled water to prepare a 0.3% working solution. The fixed cells were stained with the working solution for 1 h. After the cells were washed with distilled water, representative images were taken with a Leica ICC50 HD microscope (Leica Microsystems, Waltzer, Germany).

Immunofluorescence staining

Cells were fixed with 4% periodate-lysine-paraformaldehyde buffer for 15 min and blocked for 1 h. Primary antibodies LC3I/II (#12741; Cell Signaling Technology, Danvers, MA, USA) and perilipin1 (#4854; Vala Sciences, San Diego, CA, USA) were incubated at room temperature for 2 h. Then, secondary antibodies Alexa Fluor 555 (#4413; Cell Signaling Technology) and m-IgGBP-FITC (sc-516140; Santa Cruz Biotechnology, Texas, CA, USA) were incubated for 1 h. Images were acquired using a LSM 980 confocal microscope (Carl Zeiss Microscopy, Germany).

Western blot

Cells were lysed in RIPA buffer (#89900; Thermo Scientific, Rockford, IL, USA). Proteins (50 μg) were separated by sodium dodecyl-sulfate polyacrylamide gel electrophoresis (SDS-PAGE) and then transferred to polyvinylidene fluoride membranes. These membranes were incubated with primary antibodies at 4 °C overnight. LC3I/II (#12741), p62 (#5114), HSL (#4107), ATGL (#2138), PPARγ (#2435), C/EBPα (#8178), FABP4 (#3544), and β-tubulin (#2146) antibodies were from Cell Signaling Technology. Prohibitin (sc-377037) and anti-rabbit IgG-HRP (sc-2004) from Santa Cruz Biotechnology, PINK1 (23274-1-AP) from Proteintech (Rosemont, IL, USA), and OXPHOS (45-8099) from Invitrogen (Waltham, MA, USA) were used. Blot intensity was measured using LAS-4000 (Fuji photo film, Tokyo, Japan). Values were normalized to β-tubulin as a housekeeping protein.

Gene expression analysis

Total RNAs were extracted from the cells by using Trizol reagent (TR118; MRC, Cincinnati, OH, USA). cDNAs were synthesized using total RNAs and TOPscriptTM RT DryMIX (Enzynomics; Daejeon, South Korea). mRNA levels were observed via real-time PCR by using Rotor-Gene Q (QIAGEN; Hilden, Germany) with a 10 μl reaction volume consisting of cDNA transcripts in TOPreal SYBR Green PCR kit (Enzynomics; Daejeon, South Korea) with the following primer sets: p62 5′-AGATGC CAGAATCGGAAGGG-3′ (forward) and 5′-GAGGGA CTCAATCAGCCG-3′ (reverse); BECLIN1 5′-GCCTCT GAAACTGGACACGA-3′ (forward) and 5′-TAGCCT CTTCCTCCTGGGTC-3′ (reverse); PINK1 5′-GTGGGA CTCAGATGGCTGTC-3′ (forward) and 5′-GCACATTTG CAGCTAAGCGT-3′ (reverse); PARKIN 5′-AGCCAG

AGGTCCAGTTAAACC-3′ (forward) and 5′-TTCGAG CAGTGAGTCGCAAT-3′ (reverse); PGC1A 5′-TCGATG TGTCGCCTTCTTGC-3′ (forward) and 5′-ACGAGA GCGCATCCTTTGG-3′ (reverse); mtTFA 5′-CGTGAG ACGAACCGGACGGC-3′ (forward) and 5′-GCACAT CTCGACCCCCGTGC-3′ (reverse); mtDNA 5′-CCACTT CATCTTACCATTTA-3′ (forward) and 5′-ATCTGCATC TGAGTTTAATC-3′ (reverse); MFN1 5′-GACGGAGTG AGTGTCCGCT-3′ (forward) and 5′-TTGTGTGACCAA TCCCGCTG-3′ (reverse); DRP-1 5′- GCCTCAGATCGT CGTAGTGG-3′ (forward) and 5′-TTTTCCATGTGGCAG GGTCA-3′ (reverse); PRDX3 5′-GCGGCTGCGGGAAGG TTGCT-3′ (forward) and 5′-TGCTGGGTGACAGCAGGG GT-3′ (reverse); CPT1A 5′-ACCACTGGCCGCATGTCA AG-3′ (forward) and 5′-AGCGAGTAGCGCATAGTCAT-3′ (reverse); MnSOD 5′- GTGGTGGAGAACCCAAAGGA-3′ (forward) and 5′-AACCTTGGACTCCCACAGACA-3′ (reverse); GPX1 5′-AGTCCACCGTGTATGCCTTC-3′ (forward) and 5′-GAGAAGCGACATTCAATG-3′ (reverse); GPX2 5′-CCAAGTCGTTCTACGATCTC-3′ (forward) and 5′-CACATTCTCAATCAGCACAG-3′ (reverse); GPX3 5′-TGTGCTGTCCTAGAATGAA-3′ (forward) and 5′-CAG AAGCTTCAGCTAGTTAT-3′ (reverse); GPX4 5′-ACCAAC GTGGCCTCGCAATG-3′ (forward) and 5′-CCTGCCTCC CAAACTGGTTGC-3′ (reverse); and 18 S 5′-CGAAAGCAT TTGCCAAGAAT-3′ (forward) and 5′-AGTCGGCATCGT TTATGGTC-3′ (reverse). Gene expression levels were normalized against 18 S rRNA.

Statistical analysis

Data were statistically analyzed using Statview v5.0 (SAS Institute Inc., Cary, NC, USA) and reported as mean ± standard error of the mean of triplicate experiments. The mean values obtained from each group were compared through one-way analysis of variance (ANOVA) followed by Fisher's protected least significant difference *post hoc* test. Graphs were constructed using GraphPad Prism 8.0 (San Diego, CA, USA). $P < 0.05$ was considered statistically significant.

Results

Effects of autophagy inhibition on mitochondrial quality control in adipocytes

The protein expression of adipogenic markers was measured in preadipocytes and mature adipocytes to confirm the identity of adipocytes. PPARγ, C/EBPα, and FABP4 protein expression levels were significantly upregulated in mature adipocytes compared to preadipocytes (Fig. S1A). Oil Red O staining revealed that lipid accumulated in mature adipocytes only (Fig. S1B).

Autophagy is necessary to eliminate malfunctioning mitochondria, but excessive autophagy can result in the reduced number of mitochondria and thus the downregulation of cellular oxidative capacity. To gain insights into the effects of autophagy on mitochondrial quality control in adipocytes, we treated mature 3T3-L1 adipocytes with the autophagy inhibitor chloroquine. In differentiated 3T3-L1 adipocytes, the protein expression levels of LC3II and p62 significantly increased from 3 h after chloroquine treatment in a time-dependent manner, indicating a reduction in macroautophagy (Fig. 1A). Consistent with the protein expression, the mRNA expression level of p62 increased 6 and 24 h after chloroquine treatment (Fig. 1B), indicating that the transcriptional upregulation of p62 might also increase its protein expression (Yang et al. 2017). Interestingly, autophagy inhibition by chloroquine resulted in a decreased mitochondrial DNA (mtDNA) content from 6 h after the treatment in a time-dependent manner (Fig. 1C), implying that autophagy suppression by chloroquine induced mtDNA damage.

In search of mechanisms related to changes in mtDNA content, we measured the markers of mitophagy, mitochondrial dynamics, and mitochondrial biogenesis. The protein expression of the mitochondrial damage sensor PINK1, which is a critical regulator of mitophagy, was unchanged by chloroquine treatment (Fig. 1D). However, the gene expression levels of PINK1 and Parkin, a signal amplifier in mitochondrial polyubiquitination, significantly decreased 3 h after chloroquine treatment (Fig. 1E). Interestingly, the mRNA expression of Parkin significantly increased at 6 h, indicating the possible activation of feedback machinery. Consistent with the downregulation of mitophagy-related genes, the mitochondrial fission-related gene dynamin-related protein 1 (DRP1) also decreased at 3 h, while the mitochondrial fusion-related gene mitofusin 1 (MFN1) remained unchanged (Fig. 1F), implying a shift in the dynamic balance after chloroquine treatment. In contrast to early responses in genes related to mitophagy and dynamics, the upregulation of PGC1α, a master regulator of mitochondrial biogenesis, occurred 6 h after chloroquine treatment. This result suggested an adaptive response to restore mtDNA levels. However, after 24 h of chloroquine treatment, the gene expression levels of PGC1α and mitochondrial transcription factor A (mtTFA) significantly decreased, indicating a failure in mitochondrial biogenesis machinery. These results indicated that chloroquine-induced autophagy dysregulation altered mitochondrial homeostasis by affecting mitophagy and dynamics at an early time point while suppressing biogenesis after a long-term treatment.

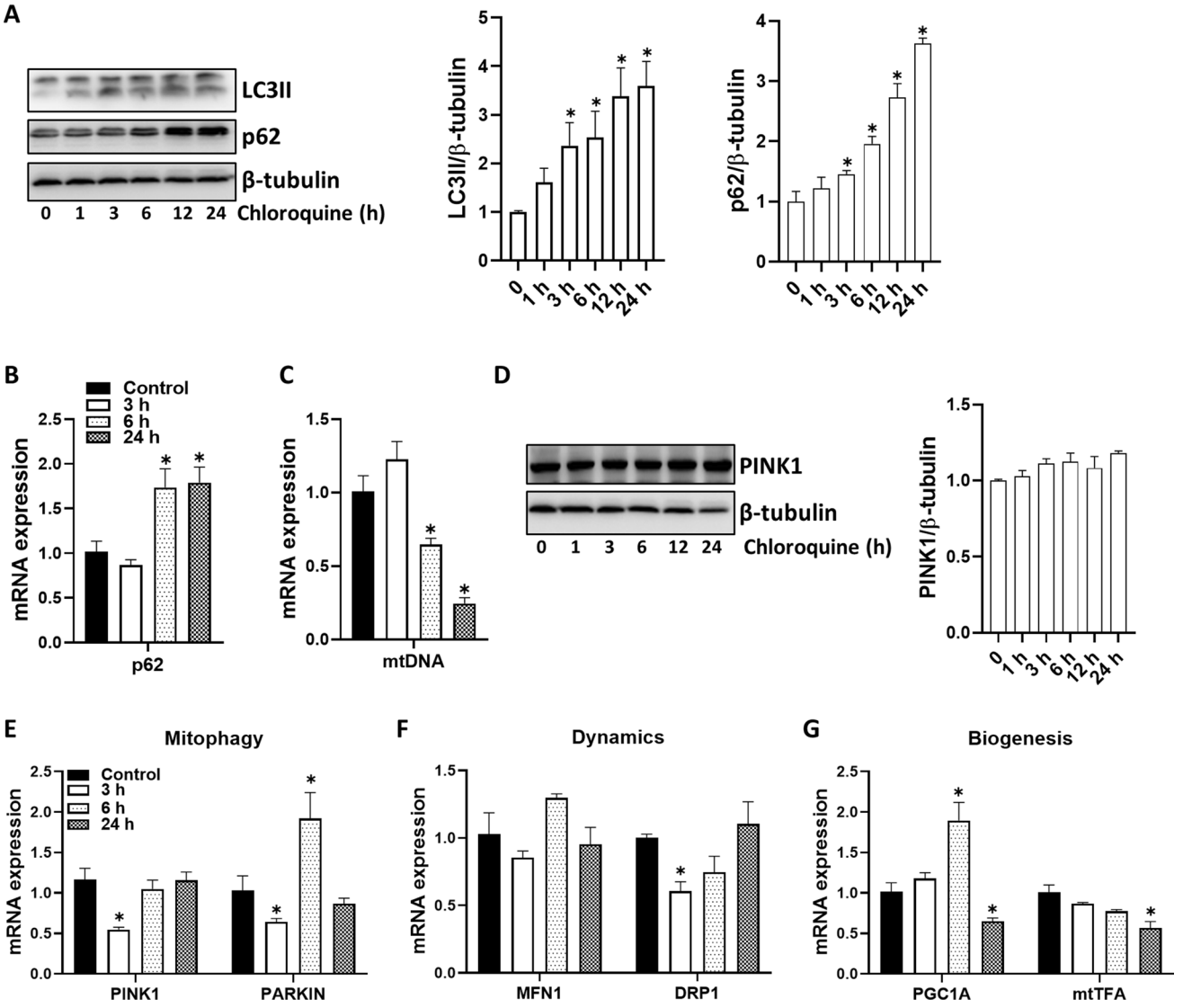

Fig. 1 Chloroquine-induced autophagy inhibition alters mitochondrial integrity. **A**, **D** Representative Western blot picture and quantification of autophagy-related proteins LC3, p62 and mitophagy-related protein PINK1. Quantifications were normalized to β-tubulin. Gene expressions of (**B**) p62 (**C**) mitochondrial DNA (**E**) mitophagy (**F**) dynamics, and (**G**) biogenesis markers were measured using real-time PCR. Quantifications were normalized to 18 S rRNA for each target. Values are presented as mean ± standard error of the mean (n = 3). * $p < 0.05$ compared with control

Effects of autophagy inhibition on mitochondrial complex expression in adipocytes

The protein expression of prohibitin was measured to examine whether mitochondrial abundancy was affected by chloroquine treatment (Fig. 2A-B). Chloroquine treatment for 48 and 72 h resulted in the upregulation of the prohibitin expression, suggesting that mitochondria accumulated because of autophagy inhibition. The mitochondria mainly produce ATP by oxidizing glucose and lipids, and oxidative phosphorylation (OXPHOS) enzymes mainly participate in the metabolic pathway (Patti and Corvera 2010). Therefore, we evaluated the abundance of OXPHOS enzymes. Normalizing the complex expression by β-tubulin expression did not result in any change by chloroquine treatment. However, normalizing their expression by prohibitin expression resulted in the downregulation of OXPHOS complex expression by chloroquine, which was more evident after 72 h treatment. These results implied that while mitochondrial mass was increased by chloroquine-mediated autophagy inhibition, OXPHOS enzymes per mitochondrion decreased, indicating deficiencies in the mitochondrial electron transport chain. Together with the reduced mtDNA levels, these observations were consistent with a decrease in mitochondrial quality.

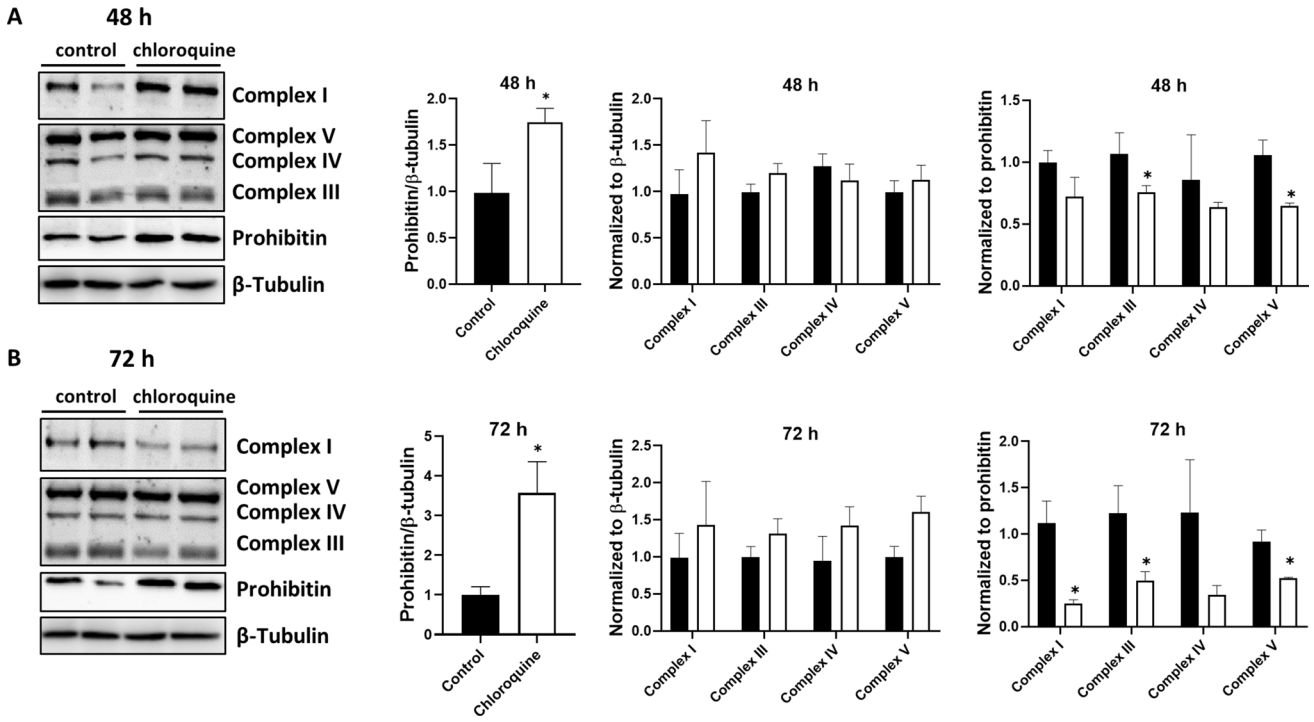

Fig. 2 Chloroquine-induced autophagy inhibition alters the oxidative phosphorylation enzyme expression. Mature adipocytes were treated with chloroquine (30 μM) for 48 and 72 h. Representative western blot picture and quantification after (**A**) 48 and (**B**) 72 h of chloroquine treatment. Quantification was either normalized to prohibitin or β-tubulin. Values are presented as mean ± standard error of the mean (n = 3). * $p < 0.05$ compared with control

Effects of autophagy inhibition on mitochondrial respiratory function in adipocytes

The metabolic function of the mitochondria was examined using the Seahorse XF analyzer 24, 48, and 72 h after chloroquine treatment in adipocytes (Fig. 3A). While the downregulation of basal respiration was only observed at 72 h (Fig. 3B), the maximal respiration and ATP production were significantly downregulated 24, 48, and 72 h after chloroquine treatment (Fig. 3C, D). Therefore, chloroquine-induced autophagy inhibition could disrupt the mitochondrial respiratory functions by altering the oxidative phosphorylation of the electron transport chain.

Effects of autophagy inhibition on redox homeostasis in adipocytes

Mitochondrial dysfunction is closely related to oxidative stress in adipocytes (Furukawa et al. 2004). Our results showed that chloroquine changed the mitochondrial genes and mitochondrial respiratory function; therefore, we examined whether this treatment affected redox homeostasis in adipocytes. H_2O_2 levels were unchanged at 24 h but were upregulated 48 and 72 h after chloroquine treatment (Fig. 4A). Along with changes in H_2O_2 levels, the total GSH significantly increased at 48 and 72 h of chloroquine treatment in adipocytes (Fig. 4B). In addition, the gene expression of glutathione peroxidases (GPXs), which downregulate H_2O_2 through a glutathione-dependent reaction (Kobayashi et al. 2009), showed that GPX3 and GPX4 were significantly upregulated while GPX1 and GPX2 gene expression remained unchanged (Fig. 4E); these results implied a compensatory increase in the glutathione system to counteract the oxidative stress by chloroquine treatment. In contrast to the increase in GSH levels, the SOD antioxidant activity was downregulated after 72 h of chloroquine treatment (Fig. 4C). Next, MnSOD activity was measured to examine whether the effect of chloroquine was mitochondrion specific. MnSOD was decreased significantly in 48 h chloroquine-treated group with a similar trend in 72 h (Fig. 4D). In addition, the gene expression of the mitochondrial antioxidant PRDX3 significantly decreased in chloroquine-treated adipocytes (Fig. 4E). Together, these results indicate a mitochondrial redox imbalance in chloroquine-treated adipocytes.

Defect in mitochondrial oxidative stress is closely related to apoptotic cell death (Ott et al. 2007). Beclin1, which plays an anti-apoptotic role, was downregulated by chloroquine treatment (Fig. 4F). The activity of the apoptotic effector caspase-3 was also induced by apoptotic cell death after 48

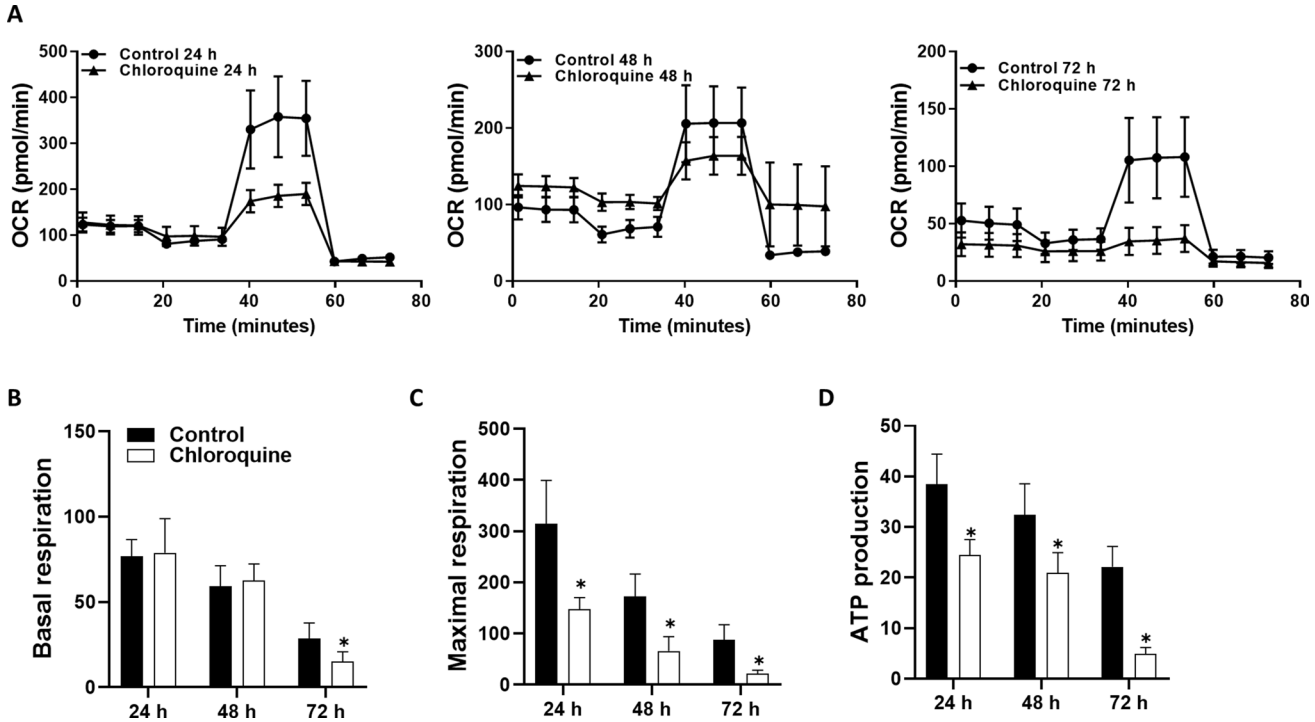

Fig. 3 Chloroquine-induced autophagy inhibition disrupts mitochondrial respiratory functions. Mature adipocytes were treated with chloroquine (30 μM) for 24, 48, and 72 h. **A** Oxygen consumption rate (OCR) for different time intervals. **B** Basal respiration, **C** maximal respiration, and **D** ATP production were calculated from Seahorse OCR values. Values are presented as mean ± standard error of the mean (n = 3). *$p < 0.05$ compared with control

and 72 h of chloroquine treatment (Fig. 4G). These results implied that chloroquine-mediated mitochondrial dysregulation was associated with oxidative stress by disrupting the mitochondrial redox balance, leading to apoptotic cell death.

Effects of autophagy inhibition on glucose uptake and lipid metabolism

Mitochondrial dysfunction in adipocytes is associated with the impairment of adipose tissue function, leading to the development of metabolic disorders (Kusminski and Scherer 2012; Lee et al. 2019). Therefore, we examined whether chloroquine-mediated mitochondrial dysregulation altered the metabolic functions of adipocytes. The gene expression of CPT1A significantly decreased after chloroquine treatment, indicating that fatty acid oxidation was suppressed (Fig. 5A). The glucose uptake activity of adipocytes was also significantly downregulated by chloroquine (Fig. 5B). Lipophagy is a distinct autophagy form, which regulates intracellular lipid stores via autophagosome-mediated triacylglycerol hydrolysis (Singh et al. 2009a). In Fig. 5C, the protein expression levels of adipose triglyceride lipase (ATGL) and total hormone-sensitive lipase (HSL) were significantly downregulated by chloroquine. For more direct evidence, co-localization of LC3 and perilipin1, a major protein implicated in adipocyte lipid droplet (LD) coating, was observed. As shown in Fig. 5D, chloroquine treatment enhanced the punctuated LC3 signal compared with that in the control, confirming the western blot results shown in Fig. 1A. Furthermore, LC3 and perilipin1 were co-localized in the chloroquine-treated group, suggesting that lipophagy could be blocked by chloroquine in adipocytes. These results imply that impairment in mitochondrial quality control by chloroquine results in metabolic dysregulation in adipocytes.

Discussion

In obesity, mitochondrial dysfunction is correlated with inflammation and increased oxidative stress. Similarly, autophagy plays a major role in the immune and metabolic function of adipose tissues. Nevertheless, studies have yet to clarify how autophagy regulates mitochondrial integrity and respiration in mature adipocytes. This study elucidated the effects of chloroquine on adipocyte mitochondrial quality control and metabolism. The results showed that autophagy inhibition by chloroquine caused the accumulation of damaged mitochondria, as evidenced by the impaired mitochondrial integrity with the decreased mtDNA and downregulation of oxidative phosphorylation. Changes in mitochondria

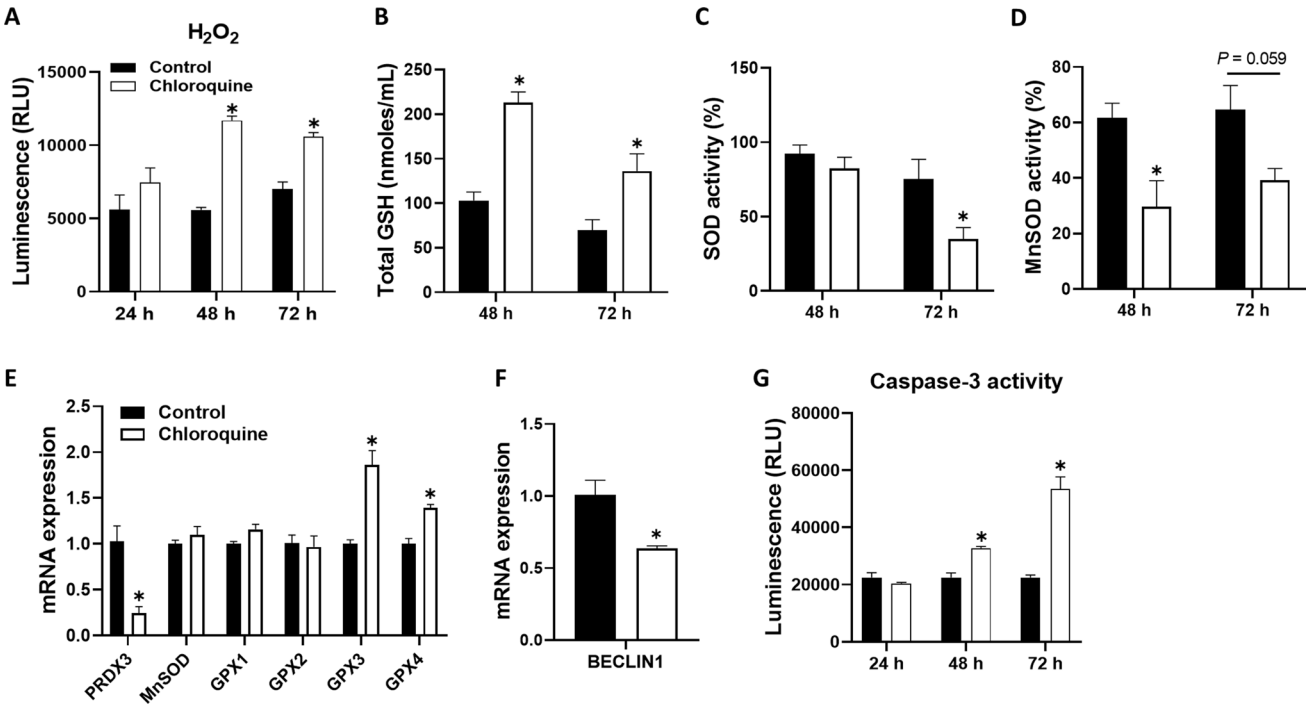

Fig. 4 Chloroquine-induced autophagy inhibition is associated with increased oxidative stress and apoptosis. Mature adipocytes were treated with 30 μM chloroquine. **A** Reactive oxygen species were measured by using hydrogen peroxide assay kit. Antioxidant activity was examined by measuring (**B**) total glutathione (GSH) level and (**C**) superoxide dismutase (SOD) activity. **D** Mitochondrial MnSOD activity was measured in the presence of potassium cyanide to deplete Cu/ZnSOD. **E**, **F** Gene expression of PRDX3, MnSOD, GPX1, GPX2, GPX3, GPX4, and BECLIN1 was measured using real-time PCR. Quantifications were normalized to 18 S rRNA levels. **G** Apoptotic cell death was measured by using caspase-3 activity kit. Values are presented as mean ± standard error of the mean (n = 3). *$p < 0.05$ compared with control

led to increased oxidative stress, apoptosis, and impaired metabolism in adipocytes.

Is autophagy advantageous or disadvantageous for adipocyte metabolism? Adipose tissue autophagy increases in human obesity and type 2 diabetes (Kovsan et al. 2011). In addition, adipose tissue phenotypes in animals that lack autophagy-related genes, including Atg5, Atg7, and Parkin, showed that mice are protected from high-fat diet-induced obesity (Baerga et al. 2009; Zhang et al. 2009; Kim et al. 2011). Further studies have shown that blocking mitophagy expands the oxidative capacity of beige adipocytes, and autophagy inhibition increases brown fat mass by controlling white adipocyte differentiation (Singh et al. 2009b); these results suggest that autophagy inhibition can be beneficial to metabolism. Conversely, the autophagy proteins Atg3 and Atg16L1 are required for proper mitochondrial function in mature adipocytes (Cai et al. 2018). Moreover, the post-developmental impairment of autophagy causes mitochondrial dysfunction, adipose inflammation, and whole-body insulin resistance (Son et al. 2020). In our study, we aimed to clarify this controversy by observing the effect of autophagy inhibition on adipocytes in a cell-autonomous manner. As a result of disruption in autophagy, the prohibitin expression increased while the mtDNA content and mitochondrial respiratory function were impaired in chloroquine-treated adipocytes, suggesting the accumulation of damaged mitochondria. These results demonstrated that autophagy is necessary for the maintenance of mitochondrial integrity in adipocytes under normal circumstances. Hence, the upregulation of autophagy markers in the adipose tissue of humans with obesity can be a compensatory response (Ferhat et al. 2019). Consistently, autophagic flux is downregulated in adipocytes from humans and animals with obesity (Soussi et al. 2015; Cai et al. 2018).

Our study has some strengths. For instance, through chloroquine treatment at various time points, we could distinguish the time-dependent effect of autophagy inhibition on adipocytes. Chloroquine treatment for 3 h downregulated the mRNA expression levels of PINK1, Parkin, and DRP1, indicating the downregulation of mitophagy and mitochondrial fission, which were important means for eliminating damaged mitochondria. PGC1α was upregulated at 6 h, implying an adaptive effort to overcome the decreased mtDNA. Despite the effort, mtDNA was further suppressed 24 h after treatment; furthermore, the PGC1α and mtTFA levels decreased, indicating an overall defect in mitochondrial integrity. The prolonged chloroquine treatment resulted in a time-dependent decrease in mitochondrial respiratory

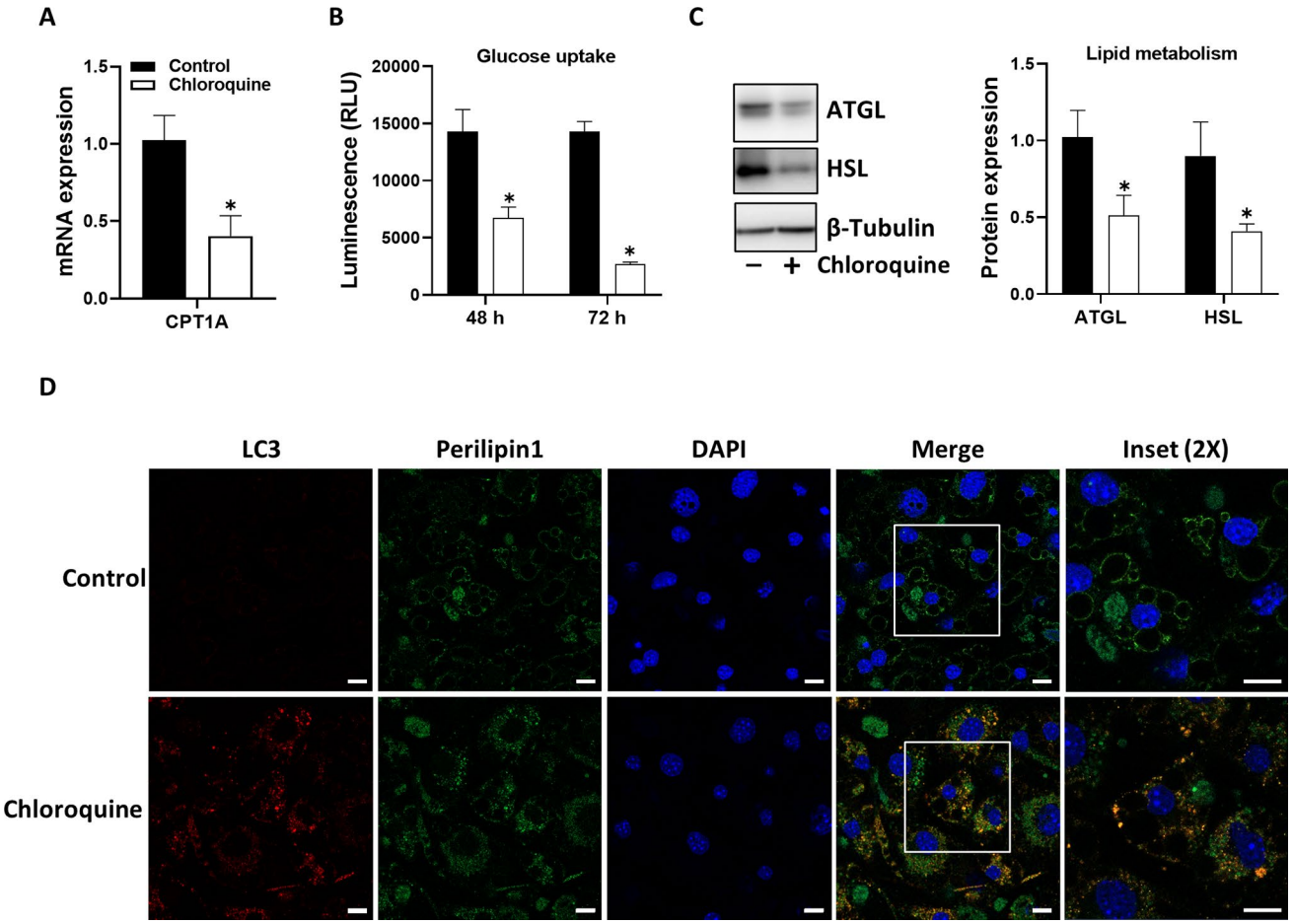

Fig. 5 Chloroquine-induced autophagy inhibition dysregulates adipocyte metabolism. Mature adipocytes were treated with 30 μM chloroquine. **A** Gene expression of CPT1A was measured using real-time PCR. Quantification was normalized to 18 S rRNA levels. **B** Glucose uptake was measured per assay kit instructions. **C** Representative Western blot picture and quantification of ATGL and HSL. Quantifications were normalized to β-tubulin. **D** Representative confocal images (scale bar = 5 μm) of LC3 (red), perilipin1 (green), and DAPI (blue). Values are presented as mean ± standard error of the mean (n = 3). * $p < 0.05$ compared with control

function, as evidenced by the decreased basal/maximal respiration and ATP production. Similarly, a tamoxifen-inducible knockout system has been utilized to identify the time-dependent effects of deletion of Beclin1, a core molecule in autophagosome formation (Son et al. 2020). While mitochondrial protein levels increased 3 days after tamoxifen induction, the loss of Beclin1 for 2 weeks resulted in the accumulation of defective autophagosomes/autolysosomes in adipocytes resembling "frustrated autophagy," thereby reducing mitochondrial content and integrity in adipose tissues. A dose-dependent effect of mitophagy has been demonstrated, and low palmitic acid (PA) concentrations induce PINK1 and Parkin to exert their protective roles, whereas high PA concentrations inhibit their expression (Cui et al. 2018). These results emphasized the importance of time- and dose-dependent responses related to autophagy regulation, which could account for controversies in various studies. Our study also has a limitation; that is, results were generated in the whole cell fraction rather than the mitochondrial fraction since white adipocytes contain a small number of mitochondria (Boudina and Graham 2014), thus making the isolation of mitochondria challenging for further analysis. To overcome the limitation and gain evidence, we provided multiple levels of data regarding mitochondria, including the gene and protein expression and activity.

Among known autophagy inhibitors, chloroquine changes the lysosomal pH, thereby inhibiting autophagic degradation in lysosomes (Homewood et al. 1972). While the direct effects of chloroquine on mitochondria have not been extensively studied in adipocytes, autophagy inhibition by chloroquine in primary neurons affects cellular bioenergetics and metabolism, consistent with decreased mitochondrial quality (Redmann et al. 2017). Notably, chloroquine induces the accumulation of p62, an autophagic cargo adapter that recruits ubiquitinated proteins and organelles to autophagosomes (Yang et al. 2017). In contrast to phenotypes observed

in Atg5 or Atg12 knockout mice, an impaired mitochondrial function in adipose tissues with decreased insulin sensitivity is observed in p62 knockout mice (Muller et al. 2013). These apparently conflicting phenotypes can be explained by the role of p62 in various signaling pathways, including those of nuclear factor κB, extracellular signal-regulated kinase 1, and nuclear factor erythroid 2-related factor 2 (Moscat and Diaz-Meco 2009; Katsuragi et al. 2015).

Chloroquine elicits detrimental effects on the mitochondria; conversely, rapamycin, a pharmacological inducer of autophagy (Sarkar et al. 2009), can ameliorate mitochondrial diseases by restoring the autophagic flux and removing damaged mitochondria (Civiletto et al. 2018; Li et al. 2018). Rapamycin also upregulates the gene and protein expression of mitochondrial biogenesis, dynamics, and mitophagy-relevant markers, thereby preventing transition from brown to white adipocytes (Huwatibieke et al. 2021). However, studies have yet to explore whether rapamycin can regulate mitochondrial bioenergetics and prevent metabolic dysregulations in an autophagy-dependent manner in adipocytes. Our results on chloroquine suggested that rapamycin would exert therapeutic effects on autophagy-mediated mitochondrial quality control in adipocytes.

The increased ROS production in adipocytes is associated with the suppression of antioxidant enzymes (Furukawa et al. 2004). Our results showed that chloroquine inhibited MnSOD but increased the total GSH levels and GPX expression. Glutathione is an intracellular antioxidant (Kwon et al. 2019), and its increase has been suggested as a compensatory response against oxidative stress in obese adipose tissues (Kobayashi et al. 2009; Ma et al. 2022). We also observed an increase in GPX3 and GPX4 expression by chloroquine treatment; this finding was consistent with our previous study, which demonstrated that GPX4 gene expression increases in response to inflammation and oxidative stress in the adipose tissue of high-fat diet mice (Ma et al. 2022). Since GPX3 and GPX4 exert protective effects on adipocytes (Lee et al. 2008; Schwarzler et al. 2022), our results implied a compensatory increase in the glutathione system to counteract mitochondrial oxidative stress by chloroquine treatment.

Interestingly, the expression levels of ATGL and HSL, which are the major enzymes responsible for lipolysis, were downregulated by chloroquine. Lipid droplet-selective autophagy, defined as lipophagy, is an essential catabolic mechanism of LD breakdown in adipocytes (Singh and Cuervo 2012). ATGL promotes lipophagy, suggesting that cytosolic lipase-dependent lipolysis and autophagy-mediated LD catabolism exhibit complementarity and cooperatively work toward lipolysis in adipose tissues and the liver (Martinez-Lopez et al. 2016; Sathyanarayan et al. 2017). Similarly, HSL phosphorylation is downregulated in Beclin1-deficient brown adipose tissue (Son et al. 2020). The authors suggested that lipophagy and cytosolic lipolysis must be simultaneously activated for an efficient lipid catabolism and LD homeostasis in vivo. Consistently, we found that an LC3-stained autophagosome and the LD protein perilipin1 were co-localized when autophagy was blocked by chloroquine, indicating that autophagy was responsible for LD degradation; this result provided further evidence supporting the connection between lipolysis and autophagy. Future studies should explore whether changes in lipolytic enzyme expression are directly or indirectly related to alterations in mitochondrial functions.

In summary, chloroquine-mediated autophagy inhibition in mature adipocytes caused defects in mitochondrial quality control and energetics, leading to oxidative stress and metabolic dysregulation. Our study expanded the current knowledge of the association of autophagy with mitochondrial function. Given that patients who took chloroquine for long periods experience ocular, cardiac, and neuro toxicities (Zou et al. 2020), our results may provide mechanistic evidence on the existence of metabolic toxicity. However, further studies should be performed to reveal the detailed mechanisms of chloroquine and other pharmacological compounds and their interplay with metabolism in adipocytes.

Acknowledgements This study was supported by the National Research Foundation of Korea (NRF) grant funded by the Korean government (MSIT) (no. 2018R1C1B6003470, 2021R1H1A1012282, 2022R1A2C1002956).

Declarations

Conflict of interest The authors declare that they have no conflicts of interests.

References

Altshuler-Keylin S, Shinoda K, Hasegawa Y, Ikeda K, Hong H, Kang Q, Yang Y, Perera RM, Debnath J, Kajimura S (2016) Beige adipocyte maintenance is regulated by autophagy-induced mitochondrial clearance. Cell Metab 24:402–419

Altshuler-Keylin S, Kajimura S (2017) Mitochondrial homeostasis in adipose tissue remodeling. Sci Signal 11(eaap527):8526

Ashrafi G, Schwarz TL (2013) The pathways of mitophagy for quality control and clearance of mitochondria. Cell Death Differ 20:31–42

Baerga R, Zhang Y, Chen PH, Goldman S, Jin S (2009) Targeted deletion of autophagy-related 5 (atg5) impairs adipogenesis in a cellular model and in mice. Autophagy 5:1118–1130

Bhatti JS, Bhatti GK, Reddy PH (2017) Mitochondrial dysfunction and oxidative stress in metabolic disorders—a step towards mitochondria based therapeutic strategies. Biochim Biophys Acta Mol Basis Dis 1863:1066–1077

Boudina S, Graham TE (2014) Mitochondrial function/dysfunction in white adipose tissue. Exp Physiol 99:1168–1178

Cai J, Pires KM, Ferhat M, Chaurasia B, Buffolo MA, Smalling R, Sargsyan A, Atkinson DL, Summers SA, Graham TE, Boudina S (2018) Autophagy ablation in adipocytes induces insulin

resistance and reveals roles for lipid peroxide and Nrf2 signaling in adipose-liver crosstalk. Cell Rep 25:1708–1717
Civiletto G, Dogan SA, Cerutti R, Fagiolari G, Moggio M, Lamperti C, Beninca C, Viscomi C, Zeviani M (2018) Rapamycin rescues mitochondrial myopathy via coordinated activation of autophagy and lysosomal biogenesis. EMBO Mol Med 10(11):e8799
Clemente-Postigo M, Tinahones A, El Bekay R, Malagon MM, Tinahones FJ (2020) The role of autophagy in white adipose tissue function: implications for metabolic health. Metabolites 10(5):179
Coban C (2020) The host targeting effect of chloroquine in malaria. Curr Opin Immunol 66:98–107
Cui C, Chen S, Qiao J, Qing L, Wang L, He T, Wang C, Liu F, Gong L, Chen L, Hou X (2018) PINK1-Parkin alleviates metabolic stress induced by obesity in adipose tissue and in 3T3-L1 preadipocytes. Biochem Biophys Res Commun 498:445–452
Ferhat M, Funai K, Boudina S (2019) Autophagy in adipose tissue physiology and pathophysiology. Antioxid Redox Signal 31:487–501
Furukawa S, Fujita T, Shimabukuro M, Iwaki M, Yamada Y, Nakajima Y, Nakayama O, Makishima M, Matsuda M, Shimomura I (2004) Increased oxidative stress in obesity and its impact on metabolic syndrome. J Clin Invest 114:1752–1761
Galluzzi L, Kepp O, Trojel-Hansen C, Kroemer G (2012) Mitochondrial control of cellular life, stress, and death. Circ Res 111:1198–1207
Galluzzi L, Bravo-San Pedro JM, Levine B, Green DR, Kroemer G (2017) Pharmacological modulation of autophagy: therapeutic potential and persisting obstacles. Nat Rev Drug Discov 16:487–511
Homewood CA, Warhurst DC, Peters W, Baggaley VC (1972) Lysosomes, pH and the anti-malarial action of chloroquine. Nature 235:50–52
Huwatibieke B, Yin W, Liu L, Jin Y, Xiang X, Han J, Zhang W, Li Y (2021) Mammalian target of rapamycin signaling pathway regulates mitochondrial quality control of brown adipocytes in mice. Front Physiol 12:638352
Javaid HMA, Sahar NE, Zhuge DL, Huh JY (2021) Exercise inhibits NLRP3 inflammasome activation in obese mice via the anti-inflammatory effect of meteorin-like. Cells 10(12):3480
Kahn CR, Wang G, Lee KY (2019) Altered adipose tissue and adipocyte function in the pathogenesis of metabolic syndrome. J Clin Invest 129:3990–4000
Katsuragi Y, Ichimura Y, Komatsu M (2015) p62/SQSTM1 functions as a signaling hub and an autophagy adaptor. FEBS J 282:4672–4678
Kim KY, Stevens MV, Akter MH, Rusk SE, Huang RJ, Cohen A, Noguchi A, Springer D, Bocharov AV, Eggerman TL, Suen DF, Youle RJ, Amar M, Remaley AT, Sack MN (2011) Parkin is a lipid-responsive regulator of fat uptake in mice and mutant human cells. J Clin Invest 121:3701–3712
Klionsky DJ, Emr SD (2000) Autophagy as a regulated pathway of cellular degradation. Science 290:1717–1721
Kobayashi H, Matsuda M, Fukuhara A, Komuro R, Shimomura I (2009) Dysregulated glutathione metabolism links to impaired insulin action in adipocytes. Am J Physiol Endocrinol Metab 296,:E1326–E1334
Kovsan J, Bluher M, Tarnovscki T, Kloting N, Kirshtein B, Madar L, Shai I, Golan R, Harman-Boehm I, Schon MR, Greenberg AS, Elazar Z, Bashan N, Rudich A (2011) Altered autophagy in human adipose tissues in obesity. J Clin Endocrinol Metab 96:E268–E277
Kusminski CM, Scherer PE (2012) Mitochondrial dysfunction in white adipose tissue. Trends Endocrinol Metab 23:435–443
Kwon DH, Cha HJ, Lee H, Hong SH, Park C, Park SH, Kim GY, Kim S, Kim HS, Hwang HJ, Choi YH (2019) Protective effect of glutathione against oxidative stress-induced cytotoxicity in RAW 264.7 macrophages through activating the nuclear factor erythroid 2-related factor-2/Heme Oxygenase-1 pathway. Antioxidants (Basel) 8(4):82
Lebleu VS, O'connell JT, Herrera G, Wikman KN, Pantel H, Haigis K, De Carvalho MC, Damascena FM, Domingos Chinen A, Rocha LT, Asara RM, Kalluri R (2014) PGC-1alpha mediates mitochondrial biogenesis and oxidative phosphorylation in cancer cells to promote metastasis. Nat Cell Biol 16,:992–1003
Lee YS, Kim AY, Choi JW, Kim M, Yasue S, Son HJ, Masuzaki H, Park KS, Kim JB (2008) Dysregulation of adipose glutathione peroxidase 3 in obesity contributes to local and systemic oxidative stress. Mol Endocrinol 22:2176–2189
Lee JH, Park A, Oh KJ, Lee SC, Kim WK, Bae KH (2019) The role of adipose tissue mitochondria: regulation of mitochondrial function for the treatment of metabolic diseases. Int J Mol Sci 20:4924
Li Q, Gao S, Kang Z, Zhang M, Zhao X, Zhai Y, Huang J, Yang GY, Sun W, Wang J (2018) Rapamycin enhances mitophagy and attenuates apoptosis after spinal ischemia-reperfusion injury. Front Neurosci 12:865
Ma EB, Javaid HMA, Jung DH, Park JH, Huh JY, Gasdermin D (2022) Deficiency does not protect mice from high-fat diet-induced glucose intolerance and adipose tissue inflammation. Mediators Inflamm. https://doi.org/10.1155/2022/7853482
Martinez-Lopez N, Garcia-Macia M, Sahu S, Athonvarangkul D, Liebling E, Merlo P, Cecconi F, Schwartz GJ, Singh R (2016) Autophagy in the CNS and periphery coordinate lipophagy and lipolysis in the brown adipose tissue and liver. Cell Metab 23:113–127
Mauthe M, Orhon I, Rocchi C, Zhou X, Luhr M, Hijlkema KJ, Coppes RP, Engedal N, Mari M, Reggiori F (2018) Chloroquine inhibits autophagic flux by decreasing autophagosome-lysosome fusion. Autophagy 14:1435–1455
Mcwilliams TG, Muqit MM (2017) PINK1 and Parkin: emerging themes in mitochondrial homeostasis. Curr Opin Cell Biol 45:83–91
Moscat J, Diaz-Meco MT (2009) p62 at the crossroads of autophagy, apoptosis, and cancer. Cell 137:1001–1004
Muller TD, Lee SJ, Jastroch M, Kabra D, Stemmer K, Aichler M, Abplanalp B, Ananthakrishnan G, Bhardwaj N, Collins S, Divanovic S, Endele M, Finan B, Gao Y, Habegger KM, Hembree J, Heppner KM, Hofmann S, Holland J, Kuchler D, Kutschke M, Krishna R, Lehti M, Oelkrug R, Ottaway N, Perez-Tilve D, Raver C, Walch AK, Schriever SC, Speakman J, Tseng YH, Diaz-Meco M, Pfluger PT, Moscat J, Tschop MH (2013) p62 links beta-adrenergic input to mitochondrial function and thermogenesis. J Clin Invest 123:469–478
Namkoong S, Cho CS, Semple I, Lee JH (2018) Autophagy dysregulation and obesity-associated pathologies. Mol Cells 41:3–10
Ott M, Gogvadze V, Orrenius S, Zhivotovsky B (2007) Mitochondria, oxidative stress and cell death. Apoptosis 12:913–922
Patti ME, Corvera S (2010) The role of mitochondria in the pathogenesis of type 2 diabetes. Endocr Rev 31:364–395
Redmann M, Benavides GA, Berryhill TF, Wani WY, Ouyang X, Johnson MS, Ravi S, Barnes S, Darley-Usmar VM, Zhang J (2017) Inhibition of autophagy with bafilomycin and chloroquine decreases mitochondrial quality and bioenergetic function in primary neurons. Redox Biol 11:73–81
Sarkar S, Ravikumar B, Floto RA, Rubinsztein DC (2009) Rapamycin and mTOR-independent autophagy inducers ameliorate toxicity of polyglutamine-expanded huntingtin and related proteinopathies. Cell Death Differ 16:46–56
Sathyanarayan A, Mashek MT, Mashek DG (2017) ATGL promotes autophagy/lipophagy via SIRT1 to control hepatic lipid droplet catabolism. Cell Rep 19:1–9
Schwarzler J, Mayr L, Radlinger B, Grabherr F, Philipp M, Texler B, Grander C, Ritsch A, Hunjadi M, Enrich B, Salzmann K, Ran Q, Huber LA, Tilg H, Kaser S, Adolph TE (2022) Adipocyte GPX4

protects against inflammation, hepatic insulin resistance and metabolic dysregulation. Int J Obes (Lond) 46:951–959
Singh R, Kaushik S, Wang Y, Xiang Y, Novak I, Komatsu M, Tanaka K, Cuervo AM, Czaja MJ (2009a) Autophagy regulates lipid metabolism. Nature 458:1131–1135
Singh R, Xiang Y, Wang Y, Baikati K, Cuervo AM, Luu YK, Tang Y, Pessin JE, Schwartz GJ, Czaja MJ (2009b) Autophagy regulates adipose mass and differentiation in mice. J Clin Invest 119:3329–3339
Singh R, Cuervo AM (2012) Lipophagy: connecting autophagy and lipid metabolism. Int J Cell Biol. https://doi.org/10.1155/2012/282041
Son Y, Cho YK, Saha A, Kwon HJ, Park JH, Kim M, Jung YS, Kim SN, Choi C, Seong JK, Burl RB, Granneman JG, Lee YH (2020) Adipocyte-specific Beclin1 deletion impairs lipolysis and mitochondrial integrity in adipose tissue. Mol Metab 39:101005
Soussi H, Reggio S, Alili R, Prado C, Mutel S, Pini M, Rouault C, Clement K, Dugail I (2015) DAPK2 downregulation associates with attenuated adipocyte autophagic clearance in human obesity. Diabetes 64:3452–3463
Traba J, Geiger SS, Kwarteng-Siaw M, Han K, Ra OH, Siegel RM, Gius D, Sack MN (2017) Prolonged fasting suppresses mitochondrial NLRP3 inflammasome assembly and activation via SIRT3-mediated activation of superoxide dismutase 2. J Biol Chem 292:12153–12164
Van Gaal LF, Mertens IL, De Block CE (2006) Mechanisms linking obesity with cardiovascular disease. Nature 444:875–880
Yang S, Qiang L, Sample A, Shah P, He YY (2017) NF-kappaB signaling activation induced by chloroquine requires autophagosome, p62 protein, and c-Jun N-terminal Kinase (JNK) signaling and promotes tumor cell resistance. J Biol Chem 292:3379–3388
Zhang Y, Goldman S, Baerga R, Zhao Y, Komatsu M, Jin S (2009) Adipose-specific deletion of autophagy-related gene 7 (atg7) in mice reveals a role in adipogenesis. Proc Natl Acad Sci USA 106:19860–19865
Zhang C, He Y, Okutsu M, Ong LC, Jin Y, Zheng L, Chow P, Yu S, Zhang M, Yan Z (2013) Autophagy is involved in adipogenic differentiation by repressesing proteasome-dependent PPARgamma2 degradation. Am J Physiol Endocrinol Metab 305,:E530–E539
Zou L, Dai L, Zhang X, Zhang Z, Zhang Z (2020) Hydroxychloroquine and chloroquine: a potential and controversial treatment for COVID-19. Arch Pharm Res 43:765–772